A Kinetic Study on the Reaction of CHF_3 with H at High Temperatures

Kazuo Takahashi,* Yasuyuki Yamamori, and Tadaaki Inomata

Department of Chemistry, Sophia University, 7-1 Kioi-cho, Chiyoda-ku, Tokyo 102, Japan

Received: April 15, 1997; In Final Form: September 8, 1997[⊗]

The reaction of CHF_3 (HFC-23) with H atoms has been investigated by using a shock tube−atomic resonance absorption spectroscopy technique over the temperature range 1100−1350 K and the total concentration range 5.5×10^{18}−8.5×10^{18} molecules cm^{-3}. Ethyl iodide was used as a precursor of hydrogen atoms. The rate coefficient for the reaction $CHF_3 + H \rightarrow CF_3 + H_2$ (1a) was determined from the decay profiles of H-atom concentration to be $k_{1a} = 10^{-9.80\pm0.10} \exp[-(64.6 \pm 2.3)\text{ kJ mol}^{-1}/RT]$ cm^3 molecule^{-1} s^{-1} (error limits at the 1 standard deviation level), which is 50−60% smaller than the value recommended by the NIST group. The rate coefficient was also calculated with the transition-state theory (TST). Structural parameters and vibrational frequencies of the reactants and transition state required for the TST calculation were obtained from an ab initio molecular orbital (MO) calculation. The energy barrier, $E_0^{\ddagger}$, which is the most sensitive parameter in the calculation, was adjusted until the TST rate coefficient most closely matched the observed one. This fitting yielded $E_0^{\ddagger} = 59.0$ kJ mol^{-1}, in excellent accord with the barrier of 62.0 kJ mol^{-1} calculated with the ab initio MO method at the G2(MP2) level.

Introduction

Halons, bromine-containing perhalogenated carbons such as CF_3Br, CF_2BrCl, and $C_2F_4Br_2$, have been used for many years as gaseous fire-extinguishing agents. They have high fire-extinguishing abilities because of their chemical suppression mechanism, that is, bromine-containing species can catalytically remove active species from the combustion zone.[1] Due to serious concerns about ozone depletion in the stratosphere, however, the production of halons has already been prohibited and the development of alternative compounds is proceeding rapidly.

Recently, trifluoromethane (CHF_3, HFC-23) was noted as one of the candidates to replace halons. Nevertheless, its inhibition mechanism is unknown so far, due to the absence of kinetic data for high-temperature reactions in fluorocarbon combustion. As a first step in our research on the flame suppression by CHF_3, we focus on the kinetics of the reaction

$$CHF_3 + H \rightarrow CF_3 + H_2 \qquad (1a)$$

which is one of the most important inhibition reactions. The rate coefficient for reaction 1a was reported to be $k_{1a} = 10^{-19.55}T^{3.00} \exp(-35.6\text{ kJ mol}^{-1}/RT)$ cm^3 molecule^{-1} s^{-1} [2] by the NIST group, and later revised downward to be $k_{1a} = 10^{-19.83}T^{3.00} \exp(-38.9\text{ kJ mol}^{-1}/RT)$ cm^3 molecule^{-1} s^{-1}.[3] These rate coefficients are fairly uncertain because they have been estimated from the rates of the reverse reaction

$$CF_3 + H_2 \rightarrow CHF_3 + H \qquad (-1a)$$

In the present study, the forward rate coefficient for reaction (1a) was experimentally determined by using a shock tube−atomic resonance absorption spectroscopy technique over the temperature range 1100−1350 K. To evaluate the validity of the experimental results, the rate coefficient was also calculated via the transition-state theory.

Experimental Section

Shock Tube. All experiments were performed behind reflected shock waves in a diaphragmless stainless steel shock tube. This shock tube is structurally similar to that reported by Koshi et al.[4] and consists of a 19.3-cm diameter × 23.5-cm long driver section and a 6.2-cm diameter × 460-cm long test section which are separated by an aluminum piston. Each shock wave was generated by removing the piston rapidly. With this system, the inner wall of the shock tube could be spared from various contaminations because it was not exposed to atmospheric components during the experiments. The test section was evacuated by a turbomolecular pump to pressures down to 1×10^{-6} Torr, in which the residual gas was practically free from hydrocarbons. To measure the incident shock velocity, three piezoelectric pressure transducers were mounted on the shock tube wall at 25-cm intervals near the end of the test section. The temperature and pressure of the shock-heated test gas were calculated from the incident shock velocity using standard methods.

ARAS. The time-resolved concentration of H ($^2S_0$, the ground state) atoms was monitored by atomic resonance absorption spectroscopy (ARAS). A microwave discharge lamp, in which helium containing 1% hydrogen was flowing at a pressure of 4 Torr, was used as a light source of H-ARAS. The resonant radiation ($^2P_{1/2}$−$^2S_0$, 121.6 nm) from the lamp passed through two MgF_2 windows (1-mm thickness) mounted on the shock tube walls at a position 2 cm from the end plate. The transmitted light was isolated by a 20-cm vacuum ultraviolet monochromator (Minutesman 302-VM), which was evacuated to a pressure less than 4×10^{-5} Torr, and detected by a solar-blind photomultiplier tube (Hamamatsu Photonics R1459). The signal was then recorded on a digital storage oscilloscope (Hitachi VC-6165).

Measurements. Measurements of the rate coefficient for the CHF_3 + H reaction were carried out in a mixture of 2 ppm C_2H_5I−0.2% CHF_3−Ar by monitoring H-atom concentration in real time. The experimental temperature and total concentration ranges were 1100−1350 K and 5.5×10^{18}−8.5×10^{18} molecules cm^{-3}, respectively. Under the present experimental conditions, H atoms were rapidly produced through thermal decomposition of ethyl iodide. Hydrogen atoms might also have been generated due to wall contaminations or resident impurities, thus blank tests with argon alone were performed during the

* Corresponding author. Phone: +81-3-3238-3457. Fax: +81-3-3238-3478. E-mail: takaha-k@hoffman.cc.sophia.ac.jp.

[⊗] Abstract published in *Advance ACS Abstracts,* November 1, 1997.

S1089-5639(97)01300-5 CCC: $14.00 © 1997 American Chemical Society

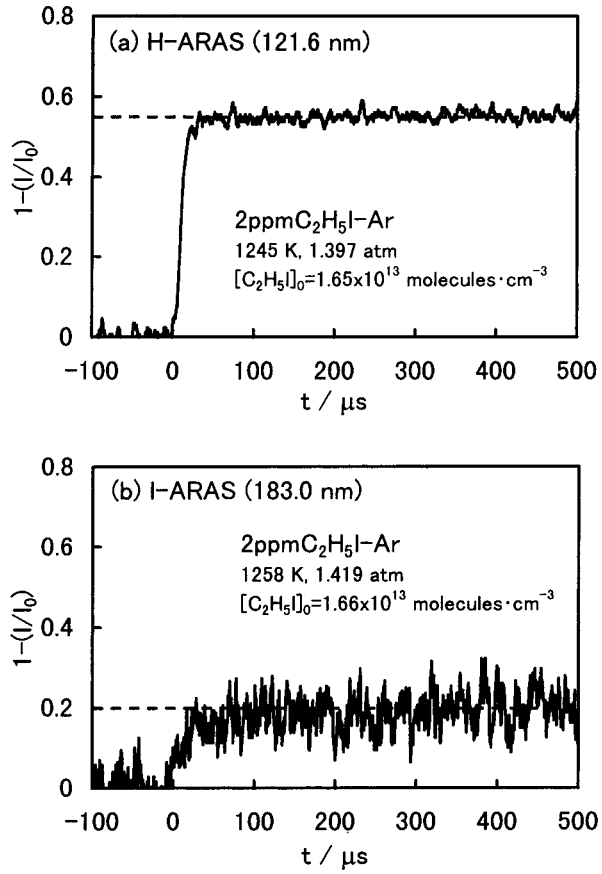

Figure 1. Typical atomic absorption profiles in 2 ppm C_2H_5I-Ar mixture. (a) H-ARAS signal at 121.6 nm. (b) I-ARAS signal at 183.0 nm. $t = 0$ denotes the arrival of reflected shock wave at the observation station of ARAS.

measurements, confirming the absence of background signals. Calibration for H-ARAS was performed in mixtures of 0.5−4 ppm C_2H_5I diluted in argon by monitoring both H and I atoms. For the thermal decomposition of ethyl iodide, as mentioned later, equimolecular amounts of H and I atoms are formed. The absolute concentration of iodine atoms was determined by I-ARAS ($^4P_{5/2}-^2P_{3/2}$, 183.0 nm), for which the calibration was previously discussed.[5]

Gases. High purity helium (99.995%) was used as the driver gas. Scientific grade argon (99.9999%) was the diluent gas. Ethyl iodide (99.0%) was purified by trap-to-trap distillation, while trifluoromethane (99.95%) was used without further purification.

Results

Calibration for H-ARAS. The calibration experiments for H-ARAS were performed in mixtures of C_2H_5I highly diluted in argon. A typical absorption profile of H atoms at 121.6 nm is shown in Figure 1a. Immediately after the arrival of a reflected shock wave, the absorption of H atoms rapidly rises to reach a nearly constant value. At temperatures above 1100 K, ethyl iodide is decomposed via two channels:

$$C_2H_5I \rightarrow C_2H_5 + I \qquad (2a)$$

$$C_2H_5I \rightarrow C_2H_4 + HI \qquad (2b)$$

Subsequently, the ethyl radical produced through reaction 2a rapidly decays to become ethylene and hydrogen atom.

$$C_2H_5 (+ M) \rightarrow C_2H_4 + H (+ M) \qquad (-3)$$

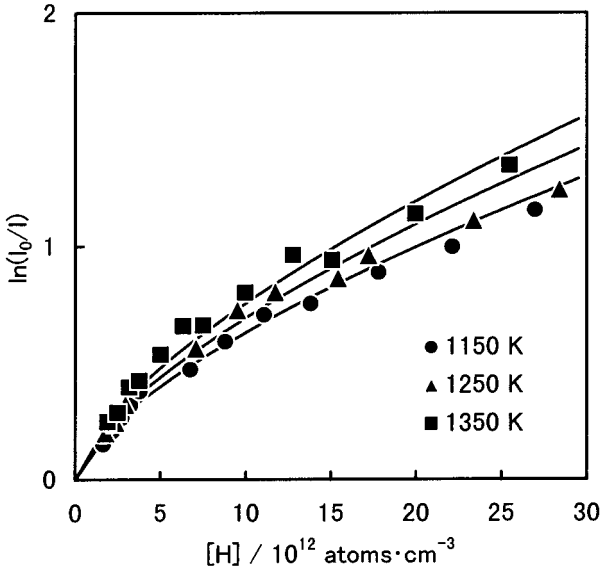

Figure 2. Calibration curves for H-ARAS at $T =$ (●) 1150, (▲) 1250, and (■) 1350 K. Three solid lines denote the curves fitted by the least-squares method (see text).

Wintergerst and Frank[6] have experimentally confirmed that the ratios of H and I atoms formed via the thermal decomposition of ethyl iodide were 1.0 ± 0.1 during the reaction time, and that the ethyl iodide could be exploited as a quantitative H atom source if the absolute concentration of I atoms was found. In this work, the absorption of I atoms at 183.0 nm ($^4P_{5/2}-^2P_{3/2}$) was also monitored under the same experimental conditions as the H-ARAS measurements, as shown in Figure 1b. The comparison between parts a and b of Figure 1 shows that the sensitivity for I-ARAS is lower than that for H-ARAS. Wintergerst and Frank[6] performed the calibration with I-ARAS at 164.2 nm ($^4P_{1/2}-^2P_{3/2}$) and obtained the same sensitivity as H-ARAS. We could not calibrate with I-ARAS at 164.2 nm because CF_3I was used as a source gas of the resonance lamp and the light emitted from the excited carbon atoms overlapped with the resonance light of iodine atoms at 164.2 nm. However, the use of I-ARAS at 183.0 nm appears to give no serious error for the determination of the rate coefficient. The calibration for I-ARAS at 183.0 nm was performed previously in shock-tube experiments that employed mixtures of CH_3I-Ar and CF_3I-Ar.[5] Therefore, the calibration for H-ARAS was performed by making the H-atom absorbance correspond to the absolute I-atom concentration after both atom concentrations reached steady states.

The calibration results for H-ARAS are shown in Figure 2. The Beer−Lambert law cannot be applied in the present study. The apparent absorption coefficients, which mean the tangential slopes of the calibration curves, decrease with the H-atom concentration due to self-absorption or self-reversal. At the same H-atom concentration, the absorbance increases somewhat with the temperature, because the Doppler width of the absorption line broadens with temperature. Assuming the modified Beer−Lambert equation

$$\ln(I_0/I) = \alpha T^{\beta}[H]^{\gamma}$$

we determined values for the three parameters (α, β, and γ) by a least-squares method as follows:

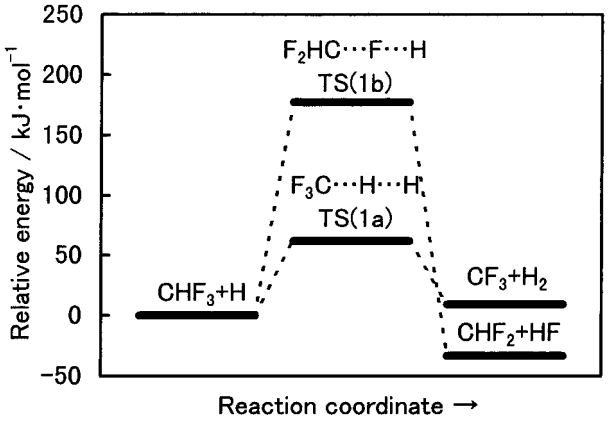

Figure 3. Energy diagram for CHF_3 + H system. The energies are calculated at the G2(MP2) level and are corrected for the zero-point vibrations.

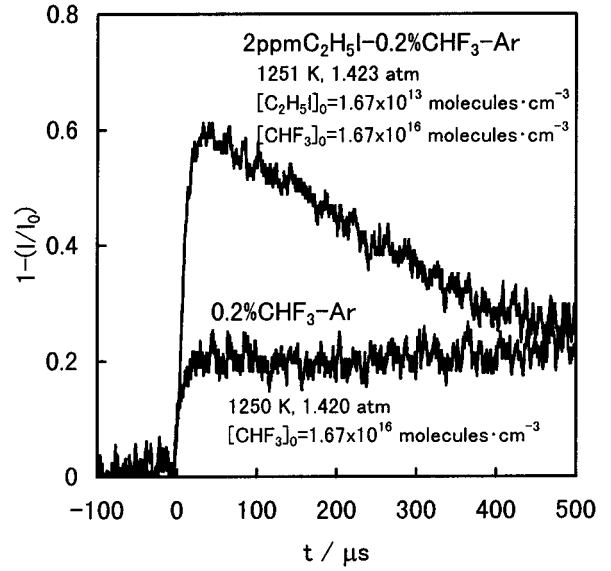

Figure 4. Typical absorption profiles at 121.6 nm in 2 ppm C_2H_5I−0.2% CHF_3−Ar and 0.2% CHF_3−Ar mixtures.

$$\alpha = 10^{-13.15\pm0.65}\ \mathrm{cm}^{1.95}\ \mathrm{atom}^{-0.65}\ \mathrm{K}^{-1.46}$$

$$\beta = 1.46 \pm 0.20$$

$$\gamma = 0.650 \pm 0.015$$

The calibration curves calculated from this expression approximate the experimental data well, as shown in Figure 2. Taking account of the light path-length for absorption, that is, the diameter of shock tube, we conclude that the sensitivity for H-ARAS measured in the present work is reasonable in comparison with the results previously reported by other workers.[7]

Rate Coefficient. The reaction of CHF_3 with H involves two competing channels

$$CHF_3 + H \rightarrow CF_3 + H_2 \qquad \Delta H^\circ_{0K} = 7.00\ \mathrm{kJ\ mol^{-1}} \quad (1a)$$

$$CHF_3 + H \rightarrow CHF_2 + HF \qquad \Delta H^\circ_{0K} = -42.2\ \mathrm{kJ\ mol^{-1}} \quad (1b)$$

where the enthalpies of formation for these chemical species, $\Delta H_f^\circ{}_{0K}$, were taken from the JANAF thermochemical tables[8] except that for CHF_2, which was taken from a NIST technical report.[2] To predict the branching ratio for the above channels, an ab initio molecular orbital (MO) calculation was performed by using the Gaussian 94 program.[9] Figure 3 shows the energy diagram for reactions 1a and 1b calculated at the G2(MP2) level.[10] The energy barrier of reaction 1b is about 115 kJ mol^{-1} higher than that of reaction 1a, although the enthalpy of reaction 1b is lower than that of reaction 1a. This difference in energy barriers means that the branching ratio, k_{1b}/k_{1a}, can be estimated to be (0.3−3.5) × 10^{-5} at 1150−1350 K, assuming that their preexponential factors are identical. Therefore, reaction 1a was estimated to be the dominant channel and reaction 1b negligible.

Measurements of the rate coefficient for the CHF_3 + H reaction were performed with a mixture of 2 ppm C_2H_5I and 2000 ppm CHF_3, diluted in argon. A typical absorption profile at 121.6 nm is shown in Figure 4 together with a profile for a mixture that did not contain C_2H_5I. Due to relatively high concentrations of CHF_3, the absorptions of not only H but also

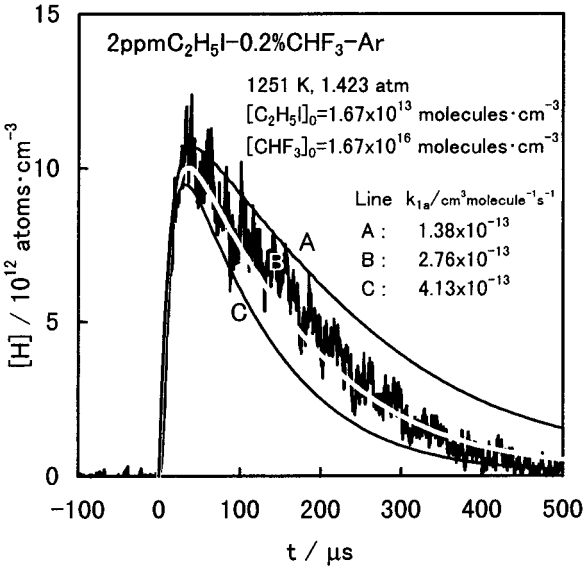

Figure 5. Typical concentration profile of H atoms in 2 ppm C_2H_5I−0.2% CHF_3−Ar mixture. Curve A, B, and C denote the profiles calculated by varying k_{1a} in the reaction scheme of Table 1.

TABLE 1: Reaction Scheme for the C_2H_5I−CHF_3 System

	reaction		forward rate coefficient[a] log A	n	E_a/R	ref
1a	$CHF_3 + H \rightarrow CF_3 + H_2$		adjusted			
2a	$C_2H_5I \rightarrow C_2H_5 + I$		11.79	0.00	20200	11
2b	$C_2H_5I \rightarrow C_2H_4 + HI$		11.11	0.00	19500	11
3	$C_2H_4 + H\ (+ M) \rightarrow C_2H_5\ (+ M)$[b]	high	−10.44	0.00	1030	12
		low	−19.76	−2.80	−24	12
4	$CHF_3 + M \rightarrow CF_2 + HF + M$		6.60	−4.00	34700	2
5	$CF_3 + H \rightarrow CF_2 + HF$		−10.04	0.00	0	2
6	$CF_2 + H \rightarrow CF + HF$		−10.40	0.00	0	13
7	$C_2H_5I + H \rightarrow C_2H_5 + HI$		−9.24	0.00	1760	1
8	$C_2H_5I + I \rightarrow C_2H_5 + I_2$		−10.18	0.00	8410	1
9	$F + F + M \rightarrow F_2 + M$		−33.56	0.00	0	1
10	$F + H + M \rightarrow HF + M$		−29.58	−1.00	0	1
11	$F_2 + H \rightarrow HF + F$		−9.70	0.00	1210	1
12	$HF + H \rightarrow H_2 + F$		−9.44	0.00	17000	1
13	$I + I + M \rightarrow I_2 + M$		−34.57	1.00	0	1
14	$I + H + M \rightarrow HI + M$		−34.48	1.00	0	1
15	$I_2 + H \rightarrow HI + I$		−9.39	0.00	0	1
16	$HI + H \rightarrow H_2 + I$		−10.26	0.00	0	1
17	$H + H + M \rightarrow H_2 + M$		−29.56	−1.00	0	12

[a] Forward rate coefficients in the form $k = AT^n \exp(-E_a/RT)$, in cm^3, molecule, s, and K units. Reverse rate coefficients were calculated from the forward ones and the equilibrium constants. [b] Pressure-dependent falloff reaction. At any pressure, the rate coefficient was calculated from $k = k_\infty[(k_0[M]/k_\infty)/(1 + k_0[M]/k_\infty)]$ where k_0 and k_∞ were low- and high-pressure limit rate coefficients, respectively.

TABLE 2: Summary of Rate Coefficients Measured for the Reaction $CHF_3 + H \rightarrow CF_3 + H_2$

		reflected shock region				
P_1[a] (Torr)	U_s[b] (m ms^{-1})	T (K)	[M] (molecules cm^{-3})	$[C_2H_5I]_0$ (molecules cm^{-3})	$[CHF_3]_0$ (molecules cm^{-3})	k_{1a} (cm^3 molecule^{-1} s^{-1})
			$[CHF_3]_0 = (1.14 \pm 0.02) \times 10^{16}$ molecules cm^{-3}			
33.0	0.748	1341	5.64×10^{18}	1.13×10^{13}	1.13×10^{16}	5.31×10^{-13}
33.0	0.744	1327	5.60×10^{18}	1.12×10^{13}	1.12×10^{16}	5.15×10^{-13}
35.0	0.721	1255	5.74×10^{18}	1.15×10^{13}	1.15×10^{16}	3.32×10^{-13}
35.0	0.718	1246	5.71×10^{18}	1.14×10^{13}	1.14×10^{16}	2.99×10^{-13}
36.0	0.706	1208	5.75×10^{18}	1.15×10^{13}	1.15×10^{16}	2.66×10^{-13}
37.0	0.690	1159	5.75×10^{18}	1.15×10^{13}	1.15×10^{16}	2.16×10^{-13}
38.0	0.667	1090	5.65×10^{18}	1.13×10^{13}	1.13×10^{16}	1.33×10^{-13}
39.0	0.653	1050	5.64×10^{18}	1.13×10^{13}	1.13×10^{16}	9.96×10^{-14}
			$[CHF_3]_0 = (1.65 \pm 0.04) \times 10^{16}$ molecules cm^{-3}			
47.0	0.749	1345	8.03×10^{18}	1.61×10^{13}	1.61×10^{16}	4.98×10^{-13}
50.0	0.737	1304	8.40×10^{18}	1.68×10^{13}	1.68×10^{16}	3.99×10^{-13}
51.0	0.720	1251	8.35×10^{18}	1.67×10^{13}	1.67×10^{16}	2.76×10^{-13}
51.0	0.717	1241	8.31×10^{18}	1.66×10^{13}	1.66×10^{16}	2.99×10^{-13}
51.0	0.709	1218	8.20×10^{18}	1.64×10^{13}	1.64×10^{16}	2.49×10^{-13}
52.0	0.704	1202	8.29×10^{18}	1.66×10^{13}	1.66×10^{16}	2.37×10^{-13}
52.0	0.695	1175	8.15×10^{18}	1.63×10^{13}	1.63×10^{16}	2.04×10^{-13}
53.0	0.687	1149	8.19×10^{18}	1.64×10^{13}	1.64×10^{16}	1.65×10^{-13}
53.0	0.677	1121	8.05×10^{18}	1.61×10^{13}	1.61×10^{16}	1.58×10^{-13}
57.0	0.653	1052	8.26×10^{18}	1.65×10^{13}	1.65×10^{16}	1.02×10^{-13}

[a] Pressure ahead of incident shock wave. [b] Incident shock velocity.

CHF_3 were found at 121.6 nm. So the net absorption of H atoms was obtained by correcting the ARAS signal with the $CHF_3-C_2H_5I-Ar$ mixture for that due to absorption by the CHF_3-Ar mixture that was obtained under the same experimental conditions. The concentration profile of H atoms determined from the net absorption is shown in Figure 5. In the presence of CHF_3, hydrogen atoms formed initially in the pyrolysis of ethyl iodide; namely, reactions 2a and -3 decay mainly through reaction 1a. The concentration profiles of H atoms were calculated by numerically integrating the rate equations in the appropriate reaction scheme of Table 1. The rate coefficient for reaction 1a, k_{1a}, was adjusted so that the calculated curve most closely matched the observed one, as shown in Figure 5. The observed rate coefficient was found to be independent of the initial concentration of CHF_3. Rate coefficient values for reaction 1a, derived under various experimental conditions, are summarized in Table 2, and the Arrhenius plot of k_{1a} is shown in Figure 6. A least-squares fit of the present experimental data yielded the following Arrhenius expression over the temperature range 1100−1350 K

$$k_{1a} = 10^{-9.80\pm0.10} \exp[-(64.6 \pm 2.3) \text{ kJ mol}^{-1}/RT] \text{ cm}^3 \text{ molecule}^{-1} \text{ s}^{-1}$$

where the error limits are given at the 1 standard deviation level. As shown in Figure 6, the present results are 50−60% smaller than the rate coefficient expression recommended in the NIST report.[3]

To evaluate the validity of the experimental results, the rate coefficient for reaction 1a was also calculated via the transition-state theory (TST). The TST rate coefficient, $k_{1a}{}^{TST}$, can be expressed as follows

$$k_{1a}{}^{TST} = \Gamma l^{\ddagger} \frac{k_B T}{h} \frac{Q^{\ddagger}}{Q_{CHF_3} Q_H} \exp\left[-\frac{E_0{}^{\ddagger}}{RT}\right]$$

where Γ is a correction factor for quantum mechanical tunneling, $l^{\ddagger}$ is the reaction path degeneracy, $E_0{}^{\ddagger}$ is the energy barrier at 0 K, and the Q's are the partition functions. k_B and h are the Boltzmann and Planck constants, respectively. All parameters required for the TST calculation are summarized in Table 3.

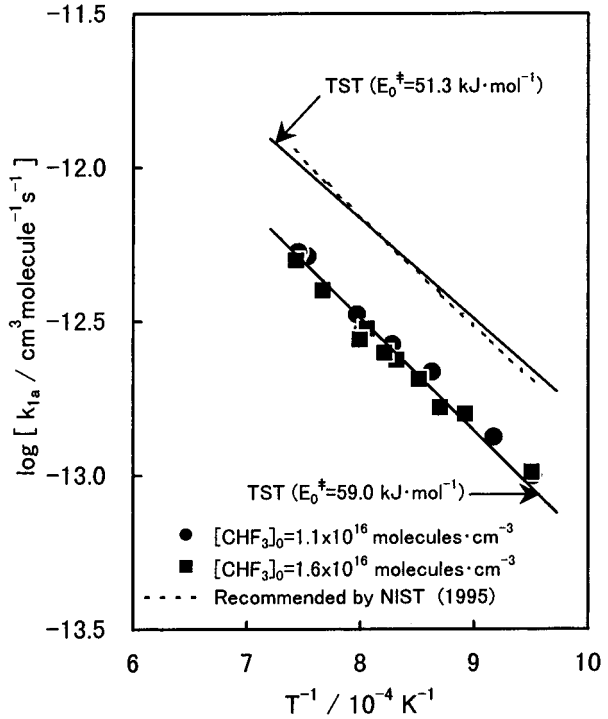

Figure 6. Arrhenius plot of the rate coefficient (k_{1a}) for the reaction $CHF_3 + H \rightarrow CF_3 + H_2$. (●) Present results measured at $[CHF_3]_0 = 1.1 \times 10^{16}$ molecules cm^{-3}. (■) Present results measured at $[CHF_3]_0 = 1.6 \times 10^{16}$ molecules cm^{-3}. (- - -) Recommendation by the NIST group.[3] (—) Results of TST calculation.

The geometries for the reactants and transition state were determined by an ab initio MO calculation at the MP2(full)/6-31G(*d*) level. The vibrational frequencies were computed at the HF/6-31G(*d*) level and scaled by a factor of 0.8929[14] to compensate for known systematic errors. Γ was roughly estimated by using the Wigner expression[15] based on the imaginary frequency for motion along the reaction coordinate, ν_i, because the tunneling effect was not large under the present conditions.

$$\Gamma \approx 1 - \frac{1}{24}\left(\frac{h\nu_i}{k_B T}\right)^2 \left(1 + \frac{k_B T}{E_0{}^{\ddagger}}\right)$$

TABLE 3: TST Calculation Parameters for the Reaction $CHF_3 + H \rightarrow CF_3 + H_2$

	reactant		transition state
	CHF_3	H	TS(1a)
molecular weight, g mol^{-1}	70.014	1.008	71.022
spin multiplicity	singlet	doublet	doublet
$E_0^{\ddagger}$, kJ mol^{-1}			adjusted
$l^{\ddagger}$			1
structural parameters			
point group	C_{3v}		C_{3v}
r(H′−H), Å			0.879
r(C−H), Å	1.089		1.423
r(C−F), Å	1.343		1.332
θ(H′−H−C), deg			180.0
θ(H−C−F), deg	110.5		108.8
θ(F−C−F), deg	108.4		110.1
moments of inertia			
I_a, g cm^2	8.213×10^{-39}		9.491×10^{-39}
I_b, g cm^2	8.213×10^{-39}		9.491×10^{-39}
I_c, g cm^2	1.498×10^{-38}		1.505×10^{-38}
vibrational frequencies, cm^{-1}	3036		2147*i*
	1414 (2)		1441
	1186 (2)		1302 (2)
	1127		1146 (2)
	681		1005
	492 (2)		662
			496 (2)
			271 (2)

The energy barrier, $E_0^{\ddagger}$, which is the most sensitive parameter in the calculation, was adjusted until the TST rate coefficients most closely matched our experimental results and the values recommended by the NIST group.[3] These TST rate coefficients are drawn with two solid lines in Figure 6. The fitting to our experimental results yielded $E_0^{\ddagger} = 59.0$ kJ mol^{-1}, in excellent accord with the barrier of 62.0 kJ mol^{-1} calculated with the ab initio MO method at the G2(MP2) level.[10] In contrast, the fitting to the NIST's recommended value led to $E_0^{\ddagger} = 51.3$ kJ mol^{-1}, which was beyond the limits of the average absolute deviation at the G2(MP2) level.

Discussion

In the present study, we first tried to derive k_{1a} directly from the following equation

$$k_{1a} = -\frac{1}{\Phi_{2a}[CHF_3]_0[C_2H_5I]_0}\left.\frac{d[H]}{dt}\right|_{t=0}$$

where Φ_{2a} is the branching ratio, $k_{2a}/(k_{2a} + k_{2b})$. This equation can be applied on the assumptions that (i) the production of hydrogen atoms from ethyl iodide is completed immediately at $t = 0$ and (ii) the competitive reactions for H-atom consumption are negligible. However, these two assumptions could not be satisfied simultaneously in the present system. The times when 99% of hydrogen atoms are formed through the reaction sequence, reactions 2a and −3, are estimated to be 512 μs at 1100 K and 32 μs at 1300 K, respectively, which are too long to derive k_{1a} directly from the above equation. At temperatures above 1500 K, although the formation rate of H atoms is fast enough, reaction 4 and its subsequent reaction 6 become a dominant pathway for H-atom consumption instead of the focus reaction 1a.

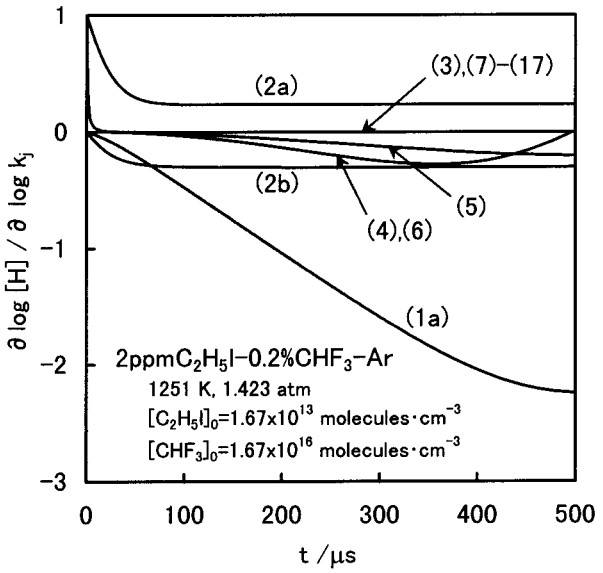

Figure 7. Sensitivity analysis of the rate coefficients for H-atom concentration in 2 ppm C_2H_5I−0.2% CHF_3−Ar mixture. Numbers in the figure denote the reaction numbers given in Table 1.

$$CHF_3 + M \rightarrow CF_2 + HF + M \quad (4)$$

$$CF_2 + H \rightarrow CF + HF \quad (6)$$

So the rate coefficient for reaction 1a had to be determined indirectly by fitting the H-atom concentration profiles calculated by using the reaction scheme proposed in Table 1 to the observed ones. To check the influence of reactions 2−17 on the determination of k_{1a}, sensivity analyses were made by using the CHEMKIN-II[16] and SENKIN[17] program codes. Typical time-resolved profiles of the normarized first-order sensitivity coefficients for H-atom concentration, $\partial(\log [H])/(\partial \log k_j)$, are shown in Figure 7. The calculation shows that reaction 1a is most sensitive for H-atom concentration and that the present experimental conditions are suitable to derive k_{1a}. In contrast, the concentration of H atoms will never be affected by reactions 3 and 7−17. The kinetic data cited for reactions 2a and 2b have been directly measured by using a shock tube−ARAS technique.[11] Even if they are not accurate, these rate coefficients cannot create a large error in the determination of k_{1a}. The sensitivity coefficients for reactions 4−6 are also not 0, but they are very small. For example, an uncertainty of ±50% for k_4−k_6 only causes an error of 3−5% to k_{1a} at 1250 K. Therefore, we can conclude that k_{1a} has no serious error due to the uncertainty of kinetic data for these side reactions.

The TST calculation yielded $E_0^{\ddagger} = 59.0$ kJ mol^{-1} from fitting to our measured rate coefficient, in excellent accord with the barrier of 62.0 kJ mol^{-1} calculated with the G2(MP2) theory.[10] In contrast, the fitting to the NIST's recommendation values[3] led to $E_0^{\ddagger} = 51.3$ kJ mol^{-1}. Curtiss et al.[10] reported that the average absolute deviation was ±6.61 kJ mol^{-1} for various

TABLE 4: Comparison of Rate Coefficients for the Reactions $CH_nF_{4-n} + H \rightarrow CH_{n-1}F_{4-n} + H_2$

		D^0_{298K}(C−H)		rate coefficient at 1250 K	
reaction	$l^{\ddagger}$	(kJ mol^{-1})	ref	(cm^3 molecule^{-1} s^{-1})	ref
$CH_3F + H \rightarrow CH_2F + H_2$	3	423.8	18	1.0×10^{-12}	20
$CH_2F_2 + H \rightarrow CHF_2 + H_2$	2	431.8	19	5.6×10^{-13}	21
$CHF_3 + H \rightarrow CF_3 + H_2$	1	446.4	19	3.2×10^{-13}	this work
				6.9×10^{-13}	3

relative energies calculated at the G2(MP2) level. In the present study, the enthalpy of reaction 1a was calculated to be 9.42 kJ mol^{-1} at the G2(MP2) level, of which the absolute deviation from the experimental data was only 2.42 kJ mol^{-1}. This excellent agreement shows that the G2(MP2) energies for the $CHF_3 + H$ system can be calculated with a high accuracy and that the $E_0^{\ddagger}$ value obtained from fitting to the NIST recommendation is too small.

Several kinetic studies on the reactions of other fluoromethanes with hydrogen atoms have been previously performed at high temperatures. The rate coefficients for the reactions $CH_nF_{4-n} + H \rightarrow CH_{n-1}F_{4-n} + H_2$ at 1250 K are summarized in Table 4 together with the reaction path degeneracies, $l^{\ddagger}$'s, and the dissociation energies of C−H bonds, D^0_{298K}(C−H)'s. Taking the present value for k_{1a}, these rate coefficients appear to increase as the number of abstractable H atoms from the fluorocarbons becomes larger and as the dissociation energies of the C−H bonds become smaller. In contrast, the NIST recommendation for k_{1a} does not fit this simple trend. Therefore, we conclude that the rate coefficient for reaction 1a determined in the present study is more reasonable than the NIST recommendation.

Acknowledgment. The authors express their gratitude to Professor Frank Scott Howell S. J. for his valuable comments.

References and Notes

(1) Westbrook, C. K. *Nineteenth Symposium (International) on Combustion*; The Combustion Institute: Pittsburgh, 1982; p 127.

(2) Nyden, M. R.; Linteris, G. T.; Burgess, D. R. F.; Westmoreland, P. R.; Tsang, W.; Zachariah, M. R. NIST SP 861; NIST: Washington, D.C., 1994; p 467.

(3) Burgess, D. R. F.; Zachariah, W.; Tsang, W.; Westmoreland, P. R. NIST Technical Note 1412; NIST: Washington, D.C., 1995.

(4) Koshi, M.; Yoshimura, M.; Fukuda, K.; Matsui, H. *J. Chem. Phys.* **1990**, *93*, 8703.

(5) Takahashi, K.; Inoue, A.; Inomata, T. *Twentieth Symposium (International) on Shock Waves*; World Scientific: New Jersey, 1995; p 959.

(6) Wintergerst, K.; Frank, P. *Nineteenth Symposium (International) on Shock Waves*, Vol. II; Springer: Berlin, 1993; p 77.

(7) Just, Th. In *Shock Waves in Chemistry*; Lifshitz, A., Ed.; Marcel Dekker: New York, 1981; p 279.

(8) Chase, M. W., Jr.; Davies, C. A.; Downey, J. R., Jr.; Frurip, D. J.; McDonald, R. A.; Syverud, A. N. *JANAF Thermochemical Tables*, 3rd ed.; *J. Phys. Chem. Ref. Data* **1985**, *14*, Suppl. 1.

(9) Frisch, M. J.; Trucks, G. W.; Schlegel, H. B.; Gill, P. M. W.; Johnson, B. G.; Robb, M. A.; Cheeseman, J. R.; Keith, T.; Petersson, G. A.; Montgomery, J. A.; Raghavachari, K.; Al-Laham, M. A.; Zakrzewski, V. G.; Ortiz, J. V.; Foresman, J. B.; Cioslowski, J.; Stefanov, B. B.; Nanayakkara, A.; Challacombe, M.; Peng, C. Y.; Ayala, P. Y.; Chen, W.; Wong, M. W.; Andres, J. L.; Replogle, E. S.; Gomperts, R.; Martin, R. L.; Fox, D. J.; Binkley, J. S.; Defrees, D. J.; Baker, J.; Stewart, J. P.; Head-Gordon, M.; Gonzalez, C.; Pople, J. A. *Gaussian 94W, Revision D.3*; Gaussian, Inc.: Pittsburgh, PA, 1995.

(10) Curtiss, L. A.; Raghavachari, K.; Pople, J. A. *J. Chem. Phys.* **1993**, *98*, 1293.

(11) Okada, K. Master Thesis, Sophia University, 1996.

(12) Miller, J. A.; Bowman, C. T. *Prog. Energy Combust. Sci.* **1989**, *15*, 287.

(13) Tsang, W.; Hampson, R. F. *J. Phys. Chem. Ref. Data* **1986**, *15*, 1087.

(14) Foresman, J. B.; Frisch, M. J. *Exploring Chemistry with Electronic Structure Methods*, 2nd ed.; Gaussian, Inc.: Pittsburgh, PA, 1996; p 64.

(15) Shavitt, I. *J. Chem. Phys.* **1959**, *31*, 1359.

(16) Kee, R. J.; Rupley, F. M.; Miller, J. A. Chemkin-II: A Fortran Chemical Kinetics Package for the Analysis of Gas-Phase Chemical Kinetics. Sandia National Laboratories Report SAND89-8009; Sandia Laboratories: Albuquerque, NM, 1993.

(17) Lutz, A. E.; Kee, R. J.; Miller, J. A. SENKIN: A Fortran Program for Predicting Homogeneous Gas-Phase Chemical Kinetics with Sensitivity Analysis. Sandia National Laboratories Report SAND87-8248; Sandia Laboratories: Albuquerque, NM, 1991.

(18) Pickard, J. M.; Rodgers, A. S. *Int. J. Chem. Kinet.* **1983**, *15*, 569.

(19) McMillen, D. F.; Golden, D. M. *Annu. Rev. Phys. Chem.* **1982**, *33*, 493.

(20) Baulch, D. L.; Duxbury, J.; Grant, S. J.; Montague, D. C. Evaluated kinetic data for high-temperature reactions. Volume 4. Homogeneous gas phase reactions of halogen- and cyanide- containing species. *J. Phys. Chem. Ref. Data* **1981**, *10*, Suppl. 1.

(21) Ridley, B. A.; Davenport, J. A. *J. Chem. Phys.* **1972**, *57*, 520.